



Volumetric and Compressibility Behaviour of Some Non-Electrolytes in Aqueous Solutions at 298.15 and 308.15 K

SUDHAKAR S. DHONDGE^{1*}, ANIL A. BHALEKAR², MURLIDHAR V. KAULGUD² and BHIMRAO R. TEMBHURNE²

¹Post Graduate Department of Chemistry, S.K. Porwal College, Kamptee, Nagpur-441 002, India

²Department of Chemistry, R.T.M. Nagpur University, Nagpur-440 033, India

*Corresponding author: E-mail: s_dhondge@hotmail.com

(Received: 12 May 2011;

Accepted: 15 December 2011)

AJC-10845

The experiential data for density (ρ) and speed of sound (u) have been obtained for aqueous solutions of acetonitrile, dimethyl formamide, dimethyl sulphoxide, dioxane, ethylene diamine, ethylene glycol, pyridine and tetrahydro furan at 298.15 and 308.15 K. The data have been processed to compute the derived parameters such as isentropic compressibility of solution (β_s), apparent molar volume of solute (ϕ_v) and apparent molar isentropic compressibility of solute (ϕ_{ks}). The results obtained have been interpreted in terms of solute-solvent and solute-solute interactions and hydrogen bonding between dissolved solutes and solvent molecules.

Key Words: Density, Speed of sound, Isentropic compressibility, Solute-solute interactions, Aqueous solutions of liquids.

INTRODUCTION

The study of thermodynamic properties of aqueous solutions of model compounds has always created an interest in the minds of chemists, as it is difficult to draw a conclusion about nature of interactions taking place between water and macromolecules as solutes. The thermodynamic properties of some model compounds have been studied extensively¹⁻⁵. In our laboratory we have studied thermodynamic properties of aqueous solutions of amines, alcohols, carbohydrates, *etc.*, at different temperatures⁶⁻¹². The thermodynamic properties of aqueous solutions of solutes with different functional groups have also been studied at lower temperatures¹³⁻¹⁵. At lower temperature the water is in highly ordered state. So it was considered that it will be interesting to study the aqueous solutions of acetonitrile (ACN), dimethyl formamide (DMF), dimethyl sulphoxide (DMSO), dioxane (DO), ethylene diamine (EDA), ethylene glycol (EG), pyridine (PY) and tetrahydro furan (THF) at higher temperatures in order to understand the effect of temperature on water structure, where water structure is in relatively disordered state as compared to that at lower temperature. This would also enable us to study the difference in nature of interactions at and around temperature of maximum density and higher temperature. In this communication the experimental data for density (ρ) and speed of sound (u) of aqueous solutions of above compounds have been obtained at 298.15 and 308.15 K. The data obtained have been processed to obtain the derived parameters such as isentropic compressibility

of solution (β_s), apparent molar volume of solute (ϕ_v) and apparent molar isentropic compressibility of solute (ϕ_{ks}). The results have been interpreted in terms of solute-solvent, solute-solute and hydrogen bonding interactions.

EXPERIMENTAL

The compounds used in this work, dimethyl sulphoxide (DMSO), ethylene glycol (EG) and 1-4-dioxane (DO) and ethylene diamine (EDA) were of AR grade. N-N-Dimethyl formamide (DMF), tetrahydrofuran (THF) acetonitrile (ACN) and pyridine (PY) were of LR grade. All the solvents were purified by standard methods¹⁶. Their purity was checked by measuring densities (ρ) and speeds of sound (u) of these liquids at 298.15 K. The comparison of experimental and literature values densities (ρ) and speed of sound (u) is given in Table-1. It is observed from the above table that our experimental values of ρ and u agree well with the literature¹⁷⁻²⁷. All the solutions were prepared in doubly distilled water on molality basis. Mettler balance having uncertainty of ± 0.1 mg was used for weighing.

The density measurements were made by a calibrated density bottle (volume ≈ 50 cc). The density bottle was filled with experimental solution and kept in a thermostated bath. The temperature of experimental bath was maintained constant (± 0.02 K) by circulating water from U-10 thermostat (± 0.1 K). The density bottle was calibrated by measuring the densities of aqueous solutions of sodium chloride at 298.15 K. Our

TABLE-1
COMPARISON OF OBSERVED DENSITIES (ρ) AND SPEEDS OF SOUND (U) FOR PURE SOLUTES WITH THE LITERATURE VALUES AT 298.15 K

Compound	$\rho \times 10^{-3} / (\text{kg m}^{-3})$		u / (m s ⁻¹)	
	Experimental	Literature	Experimental	Literature
DMSO	1.09570	1.09540 ^a 1.09536 ^e	1490.8	1493.00 ^a
EDA	0.89476	0.89520 ^b	1684.0	
PY	0.97800	0.97900 ^c 0.97824 ^b	1422.8	1416.10 ^d
DO	1.02780	1.02830 ^a 1.02797 ^h	1345.3	1345.00 ^a 1346.30 ^k
DMF	0.94330	0.94390 ^a 0.94397 ^h	1465.0	1462.00 ^a 1460.20 ^k
THF	0.88790	0.88270 ^e 0.88197 ⁱ	1284.0	1288.00 ^e 1277.44 ^j
ACN	0.77680	0.77710 ^e 0.77660 ^h	1280.6	1288.00 ^e 1281.30 ^k
EG	1.11000	1.10610 ^f 1.10850 ⁱ	1652.8	1664.00 ^f

^aRef. 17, ^bRef. 18, ^cRef. 19, ^dRef. 20, ^eRef. 21, ^fRef. 22, ^gRef. 23, ^hRef. 24, ⁱRef. 25, ^jRef. 26, ^kRef. 27.

density values of aqueous solutions of sodium chloride agreed well with literature²⁸ and were reproducible to $\pm 0.1 \text{ kg m}^{-3}$.

The speeds of sound were measured for aqueous solutions of solutes using an ultrasonic interferometer (Model SI-2 M/s Dr. Steeg and Reuter, Germany) at a fixed frequency of 2 MHz and having temperature control of $\pm 0.1 \text{ K}$. The details are given elsewhere¹² Interferometer was calibrated by measuring speed of sound in doubly distilled water²⁹. The uncertainty in speed of sound measurements was better than $\pm 1.0 \text{ m s}^{-1}$.

Calculations of derived parameters: Isentropic compressibility (β_s) has been calculated using the Newton-Laplace equation,

$$\beta_s = \frac{1}{\rho u^2} \quad (1)$$

where u is speed of sound and ρ is the density of solution.

The apparent molar volume (ϕ_v) and apparent molar isentropic compressibility (ϕ_{KS}) of solutes in water as a function of its concentration were calculated by using standard equations given below,

$$\phi_v = \left(\frac{M_2}{\rho} \right) + \left\{ \frac{n_1 M_1 (\rho_0 - \rho)}{m \rho \rho_0} \right\} \quad (2)$$

$$\phi_{KS} = \left(\frac{M_2 \beta_s}{\rho} \right) + \left\{ \frac{n_1 M_1 (\beta_s \rho_0 - \beta_s^0 \rho)}{m \rho \rho_0} \right\} \quad (3)$$

where n_1 is the number of moles of solvent in 1 kg of solvent, M_1 is the molecular weight of solvent, M_2 is the molecular weight of solute, m is the molality, while β_s^0 , ρ_0 and β_s , ρ , represent the isentropic compressibility and density values for solvent and solution, respectively.

The limiting apparent molar volumes (ϕ_v^0) of solute and limiting apparent molar isentropic compressibilities (ϕ_{KS}^0) of solute were obtained by smooth extrapolation of the curves of $\phi_v - x_2$ and $\phi_{KS} - x_2$ to zero concentration, respectively, where x_2 is mole fraction of solute. However, we are aware of the

fact that the ϕ_v^0 and ϕ_{KS}^0 calculated in this work cannot be treated accurate as they have been extrapolated from higher concentration. Tables 2 and 3 are collected the data of ρ , u, β_s , ϕ_v and ϕ_{KS} at 298.15 and 308.15 K, respectively, while the limiting values of apparent molar volume of the solute (ϕ_v^0), apparent molar compressibility of solute (ϕ_{KS}^0) at different temperatures and that of apparent molar expansivity, (ϕ_E^0) and temperature coefficients of ϕ_{KS}^0 ($d\phi_{KS}^0/dT$) at 303.15 K are listed in Table-4.

The uncertainty in β_s values was of the order of $\pm 0.06 \times 10^{-11} \text{ m}^2 \text{ N}^{-1}$. The errors at lowest concentration studied for derived parameters are of the order of $\pm 0.05 \times 10^{-6} \text{ m}^3 \text{ mol}^{-1}$ and $\pm 0.3 \times 10^{-15} \text{ m}^5 \text{ N}^{-1} \text{ mol}^{-1}$ for ϕ_v and ϕ_{KS} , respectively.

RESULTS AND DISCUSSION

Fig. 1 represents the variation of density (ρ) with mole fraction of the solute (x_2) for aqueous solutions of different solutes at 298.15 K. It is observed from the above figure that for ACN + H₂O and THF + H₂O systems the density of solution decreases with increase in concentration of solute. In case of EDA + H₂O system ρ remains almost constant initially with increase in concentration of solute and then decreases with further increase in concentration of solute. It is observed that in case of DMF + H₂O system, ρ decreases slowly with increase in concentration of solute. For PY + H₂O system ρ increases slowly with increase in concentration of solute goes through a flat maxima and then decreases slowly with further increase in concentration of solute. For DO + H₂O and DMSO + H₂O systems density increases initially goes through a flat maximum and then decreases slowly with increase in concentration of solute. For EG + H₂O system it increases with increase in concentration of solute and reaches to maximum at $x_2 = 1$. Same types of trends are observed at 308.15 K.

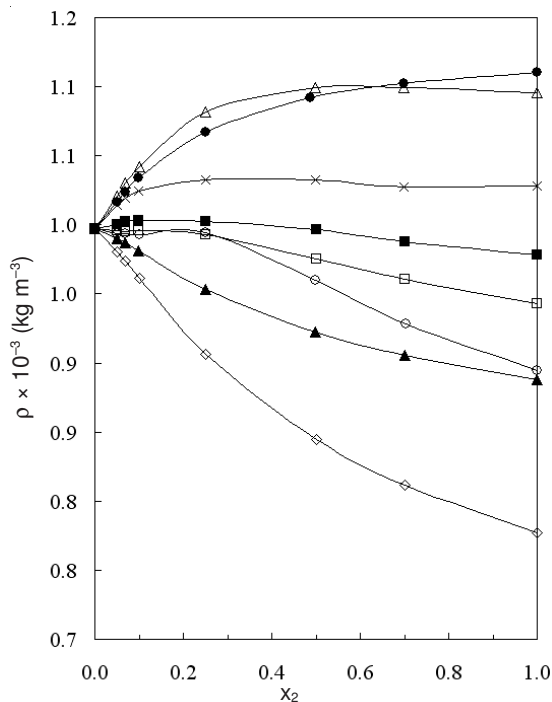


Fig. 1. Variation of density (ρ) with mole fraction of solute x_2 for aqueous systems at 298.15 K: \diamond - \diamond , ACN; \square - \square , DMF; Δ - Δ , DMSO; \times - \times , DO; \circ - \circ , EDA; \bullet - \bullet , EG; \blacksquare - \blacksquare , PY; \blacktriangle - \blacktriangle , THF

TABLE-2
 DENSITY (ρ), SPEED OF SOUND (u), ISENTROPIC COMPRESSIBILITY (β_s) OF AQUEOUS SOLUTIONS OF
 SOLUTES, APPARENT MOLAR VOLUME OF SOLUTES (ϕ_v) AND APPARENT MOLAR ISENTROPIC
 COMPRESSIBILITY (ϕ_{ks}) OF SOLUTES IN AQUEOUS SOLUTIONS AT 298.15 K

x_2	$\rho \times 10^{-3} /$ (Kg m ⁻³)	$u /$ (m s ⁻¹)	$\beta_s \times 10^{11} /$ (m ² N ⁻¹)	$\phi_v \times 10^6 /$ (m ³ mol ⁻¹)	$\phi_{ks} \times 10^{15} /$ (m ² N ⁻¹ mol ⁻¹)	x_2	$\rho \times 10^{-3} /$ (Kg m ⁻³)	$u /$ (m s ⁻¹)	$\beta_s \times 10^{11} /$ (m ² N ⁻¹)	$\phi_v \times 10^6 /$ (m ³ mol ⁻¹)	$\phi_{ks} \times 10^{15} /$ (m ² N ⁻¹ mol ⁻¹)
DMF						EG					
0.0000	0.9970	1496.8	44.77	73.57	7.72	0.0000	0.9970	1496.8	44.77	54.48	6.41
0.0502	0.9960	1598.0	39.32	73.17	10.61	0.0500	1.0165	1558.0	40.53	54.48	7.52
0.0699	0.9950	1620.0	38.30	73.95	12.93	0.0697	1.0238	1580.0	39.13	54.32	7.66
0.0999	0.9957	1646.0	37.07	73.62	14.88	0.0997	1.0337	1614.8	37.10	54.26	7.61
0.2499	0.9928	1682.0	35.60	73.85	21.36	0.2497	1.0672	1692.8	32.70	54.59	11.3
0.5004	0.9755	1597.0	40.19	75.33	29.46	0.4876	1.0920	1698.8	31.73	55.19	15.04
0.7019	0.9604	1536.0	44.13	76.40	33.67	0.6980	1.1022	1680.8	32.11	55.57	16.86
1.0000	0.9433	1465.0	49.39	–	38.27	1.0000	1.1100	1652.8	32.98	–	18.44
THF						EDA					
0.0000	0.9970	1496.8	44.77	73.97	4.48	0.0000	0.9970	1496.8	44.77	62.73	-2.97
0.0499	0.9899	1584.0	40.26	75.32	15.16	0.0503	0.9937	1638.0	37.51	61.65	-1.63
0.0699	0.9869	1586.0	40.28	75.53	19.88	0.0699	0.9937	1685.7	35.42	61.30	-0.76
0.0999	0.9815	1576.0	41.02	76.04	25.25	0.1001	0.9932	1766.7	32.26	61.14	-0.57
0.2498	0.9533	1452.0	49.76	78.13	41.63	0.2502	0.9942	1956.0	26.29	60.60	5.93
0.4998	0.9221	1352.0	59.33	79.67	49.95	0.4996	0.9595	1873.6	29.69	63.34	16.08
0.7011	0.9055	1316.0	63.77	82.16	53.86	0.7029	0.9283	1775.7	34.17	65.31	21.5
1.0000	0.8879	1284.0	68.31	–	55.39	1.0000	0.8948	1684.0	39.41	–	26.42
ACN						DO					
0.0000	0.9970	1496.8	44.77	46.47	5.58	0.0000	0.9970	1496.8	44.77	80.04	10.89
0.0500	0.9801	1550.0	42.47	47.82	12.42	0.0501	1.0142	1570.7	39.97	81.07	16.34
0.0700	0.9735	1552.0	42.65	47.98	15.38	0.0698	1.0192	1581.7	39.22	81.21	18.51
0.1008	0.9613	1544.0	43.64	48.69	19.43	0.1000	1.0248	1587.3	38.74	81.57	21.81
0.2499	0.9061	1454.0	52.20	50.74	30.52	0.2501	1.0327	1537.0	40.99	83.45	32.16
0.5000	0.8449	1358.0	64.18	51.83	36.77	0.4999	1.0329	1434.7	47.04	84.68	40.24
0.7007	0.8115	1322.0	70.51	52.35	40.74	0.6983	1.0277	1392.7	50.17	85.50	43.32
1.0000	0.7768	1280.6	78.50	–	41.43	1.0000	1.0278	1345.3	53.76	–	46.02
DMSO						PY					
0.0000	0.9970	1496.8	44.77	69.31	5.12	0.0000	0.9970	1496.8	44.77	77.25	18.62
0.0498	1.0211	1588.7	38.80	68.38	5.97	0.0497	1.0001	1548.0	41.69	77.64	21.74
0.0700	1.0303	1604.4	37.71	68.08	8.73	0.0699	1.0023	1556.0	41.21	77.65	23.44
0.1009	1.0423	1642.0	35.55	67.88	9.29	0.1000	1.0030	1563.6	40.78	77.89	25.28
0.2498	1.0814	1714.0	31.48	68.02	14.2	0.2499	1.0028	1557.6	41.10	78.57	30.31
0.4997	1.0992	1725.2	30.57	69.40	22.04	0.5004	0.9969	1514.0	43.79	79.35	34.54
0.6987	1.0990	1650.0	33.42	70.37	23.73	0.7023	0.9879	1461.6	47.38	80.14	38.17
1.0000	1.0957	1490.8	41.06	–	29.25	1.0000	0.9780	1422.8	50.51	–	40.85

In Fig. 2 showed the variations of speed of sound (u) as a function of mole fraction of solute (x_2) for aqueous solutions of the solutes studied in this work at 298.15 K. It is seen from the above figure that the speed of sound increases initially with increase in concentration of solute goes through a maximum and again decreases with increase in concentration of the solute for all the aqueous systems. However initial slopes of $u - x_2$ curves are different for different systems. It is observed that in case of EDA + H₂O the slope is highest and for DMSO + H₂O it is lowest. The slopes of the curves after maximum are more or less of same magnitude. The same type of trends of $u - x_2$ are observed for all aqueous systems studied at 308.15 K. It has been observed that at lower concentrations of solute, speed of sound increases with increase in temperature for all the aqueous systems. Whereas at higher concentrations the reverse trend is observed *i.e.* speed of sound decreases with increase in temperature. Thus there is cross over point for all the systems where temperature coefficient of speed of sound is zero ($du/dT = 0$). The concentration of cross over or cross over point is different for all the systems. For ACN + H₂O the cross over

point is at $x_2 = 0.07$. For DMF + H₂O, DMSO + H₂O, EDA + H₂O, THF + H₂O and DO + H₂O systems the crossing over takes place at $x_2 \approx 0.05$. For EG + H₂O the cross over point is at $x_2 \approx 0.12$ and for PY + H₂O it is at $x_2 \approx 0.17$. It has been observed that at lower temperatures also, speed of sound first increases with increase in concentration, goes through a maximum and then further decreases¹³⁻¹⁵.

Fig. 3 represents the variation of isentropic compressibility (β_s) of aqueous solutions of different solutes as a function of mole fraction of the solute (x_2) at 298.15 K for entire concentration range. It is observed from the above figure that β_s decreases with increase in concentration of the solute initially, goes through a minima and then further increases with increase in concentration of the solute. The initial slopes of $\beta_s - x_2$ curves are different for different systems. Highest negative initial slope is observed for EDA + H₂O system and lowest negative initial slope is observed for ACN + H₂O. The concentration of minimum of β_s is also different for different systems. Same types of graphs are obtained at 308.15 K. Initially, at lower concentration of the solute, β_s decreases with increase

TABLE-3
 DENSITY (ρ), SPEED OF SOUND (u), ISENTROPIC COMPRESSIBILITY (β_s) OF AQUEOUS SOLUTIONS OF
 SOLUTES, APPARENT MOLAR VOLUME OF SOLUTES (ϕ_v) AND APPARENT MOLAR ISENTROPIC
 COMPRESSIBILITY (ϕ_{ks}) OF SOLUTES IN AQUEOUS SOLUTIONS AT 308.15 K

x_2	$\rho \times 10^{-3} /$ (Kg m ⁻³)	$u /$ (m s ⁻¹)	$\beta_s \times 10^{11} /$ (m ² N ⁻¹)	$\phi_v \times 10^6 /$ (m ³ mol ⁻¹)	$\phi_{ks} \times 10^{15} /$ (m ⁵ N ⁻¹ mol ⁻¹)	x_2	$\rho \times 10^{-3} /$ (Kg m ⁻³)	$u /$ (m s ⁻¹)	$\beta_s \times 10^{11} /$ (m ² N ⁻¹)	$\phi_v \times 10^6 /$ (m ³ mol ⁻¹)	$\phi_{ks} \times 10^{15} /$ (m ⁵ N ⁻¹ mol ⁻¹)
DMF						EG					
0.0000	0.9940	1520.0	43.54	74.95	15.53	0.0000	0.9940	1520.0	43.54	54.93	7.61
0.0502	0.9907	1592.0	39.83	74.92	17.46	0.0500	1.0129	1578.8	39.61	54.85	8.34
0.0699	0.9900	1610.0	38.96	74.80	18.51	0.0697	1.0193	1590.0	38.81	54.90	10.04
0.0999	0.9901	1640.0	37.55	74.47	18.18	0.0997	1.0282	1620.0	37.06	54.92	9.74
0.2499	0.9846	1654.0	37.13	74.76	24.26	0.2497	1.0613	1680.8	33.35	55.03	12.81
0.5004	0.9661	1562.0	42.42	76.18	32.25	0.4876	1.0852	1683.6	32.51	55.60	16.00
0.7019	0.9514	1498.0	46.84	77.17	36.61	0.6980	1.0959	1659.7	33.13	55.91	17.75
1.0000	0.9349	1429.0	52.38	–	40.95	1.0000	1.1029	1634.7	33.93	–	19.10
THF						EDA					
0.0000	0.9940	1520.0	43.54	75.67	13.56	0.0000	0.9940	1520.0	43.54	63.01	1.82
0.0499	0.9856	1584.0	40.64	75.99	21.45	0.0503	0.9900	1636.4	37.72	62.00	3.71
0.0699	0.9818	1578.4	40.88	76.33	25.39	0.0699	0.9892	1686.8	35.53	61.81	2.92
0.0999	0.9753	1556.0	42.33	76.95	30.59	0.1001	0.9892	1756.0	32.78	61.44	2.62
0.2498	0.9449	1420.0	52.49	79.03	46.34	0.2502	0.9867	1918.0	27.55	61.21	8.18
0.4998	0.9129	1323.2	62.56	80.48	53.92	0.4996	0.9508	1829.2	31.43	63.93	18.08
0.7011	0.8953	1281.2	68.05	81.27	57.36	0.7029	0.9189	1730.0	36.36	65.92	23.64
1.0000	0.8781	1250.7	72.80	–	59.69	1.0000	0.8852	1626.0	42.73	–	28.96
ACN						DO					
0.0000	0.9940	1520.0	43.54	47.67	12.34	0.0000	0.9940	1520.0	43.54	81.22	17.63
0.0502	0.9752	1554.8	42.42	48.65	17.20	0.0501	1.0094	1570.0	40.19	81.94	21.90
0.0700	0.9671	1552.0	42.93	49.09	20.05	0.0698	1.0135	1576.7	39.69	82.18	23.81
0.1008	0.9549	1540.0	44.16	49.56	22.87	0.1000	1.0185	1577.0	39.48	82.48	25.93
0.2499	0.8996	1440.0	53.61	51.28	32.96	0.2501	1.0264	1507.0	42.90	84.02	35.70
0.5000	0.8355	1332.0	67.46	52.50	39.85	0.4999	1.0238	1395.0	50.19	85.43	44.30
0.7007	0.8007	1290.0	75.05	53.07	42.37	0.6983	1.0197	1345.3	54.18	86.10	47.71
1.0000	0.7658	1246.0	84.11	–	45.03	1.0000	1.0150	1324.0	56.2	–	48.73
DMSO						PY					
0.0000	0.9940	1520.0	43.54	70.96	10.49	0.0000	0.9940	1520.0	43.54	78.53	22.25
0.0498	1.0117	1589.6	38.92	71.10	11.96	0.0497	0.9962	1568.0	40.83	78.63	23.11
0.0700	1.0253	1613.0	37.49	68.77	11.51	0.0699	0.9963	1572.8	40.58	78.85	25.28
0.1009	1.0364	1636.4	36.03	68.70	12.63	0.1000	0.9971	1574.0	40.48	78.82	26.91
0.2498	1.0733	1685.2	32.41	68.70	16.21	0.2499	0.9962	1548.8	41.85	79.29	32.26
0.4997	1.0898	1584.0	36.57	70.03	24.42	0.5004	0.9888	1484.8	41.87	80.09	33.23
0.6987	1.0894	1515.2	39.98	70.96	28.18	0.7023	0.9789	1430.8	49.90	80.92	40.87
1.0000	1.0852	1453.6	43.61	–	31.37	1.0000	0.9679	1386.4	53.75	–	43.93

TABLE-4
 LIMITING APPARENT MOLAR VOLUMES OF SOLUTES ($\phi_v^0 = \bar{V}_2^0$) AND LIMITING APPARENT MOLAR ISENTROPIC
 COMPRESSIBILITIES OF SOLUTES (ϕ_{ks}^0) AT 298.15 K AND LIMITING APPARENT MOLAR EXPANSIVITY OF
 SOLUTES (ϕ_E^0) AND TEMPERATURE COEFFICIENT OF LIMITING APPARENT MOLAR COMPRESSIBILITY
 ($d\phi_{ks}^0/dT$) AT 303.15 K FOR AQUEOUS SOLUTIONS OF SOLUTES

	$10^6 \times \phi_v^0 / (m^3 \text{ mol}^{-1})$		$10^{15} \times \phi_{ks}^0 / (m^5 \text{ N}^{-1} \text{ mol}^{-1})$		$10^6 \times \phi_E^0 / m^3 \cdot \text{mol}^{-1} \cdot \text{K}^{-1}$		$d\phi_{ks}^0/dT$
	298.15 K	308.15 K	298.15 K	308.15 K	303.15 K	303.15K	
DMF	73.57	74.95	7.72	15.53	0.138	0.781	
THF	73.97	75.67	4.48	13.56	0.170	0.454	
ACN	46.47	47.67	5.58	12.34	0.120	0.676	
DMSO	68.38	70.96	5.97	10.49	0.285	0.452	
EG	54.48	54.93	6.41	7.61	0.045	0.12	
EDA	62.73	63.01	-2.97	1.82	0.028	0.479	
DO	80.04	81.22	10.89	17.63	0.118	0.674	
PY	77.25	78.53	18.62	22.25	0.128	0.368	

in temperature at a particular concentration for all the systems but as the concentration of solute increases a reverse trend is observed *i.e.*, a crossover takes place at a particular concentration. This crossover takes place at different concentrations for different systems. The initial decrease in β_s values is because

of loss of compressibility of water molecules attached to the solute as the number of molecules of water is much higher as compared to number molecules of solute. This also suggests strong solute-solvent interactions/hydrogen bonding between solute and solvent molecules. A strong hydrogen bonding

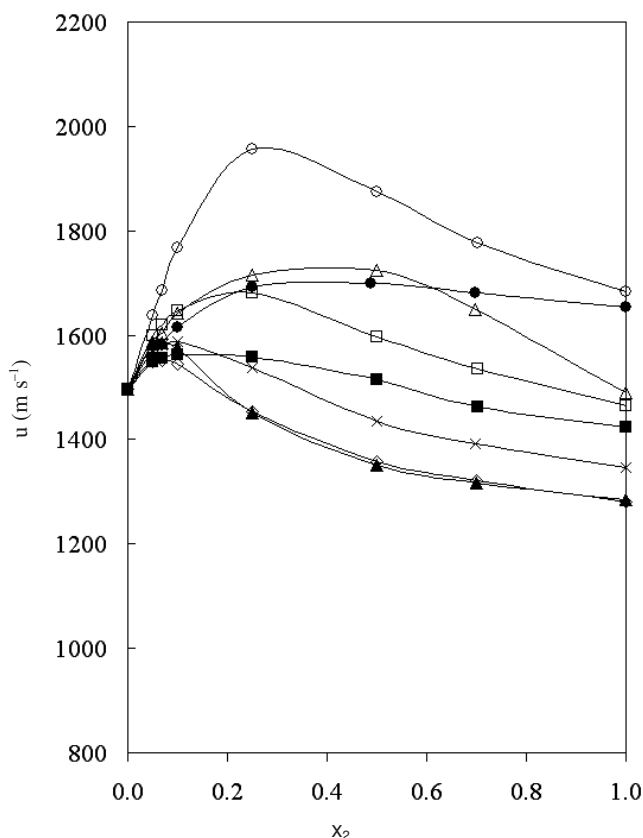


Fig. 2. Variation of speed of sound (u) with mole fraction of solute x_2 for aqueous systems at 298.15 K: \diamond - \diamond , ACN; \square - \square , DMF; Δ - Δ , DMSO; \times - \times , DO; \circ - \circ , EDA; \bullet - \bullet , EG; \blacksquare - \blacksquare , PY; \blacktriangle - \blacktriangle , THF

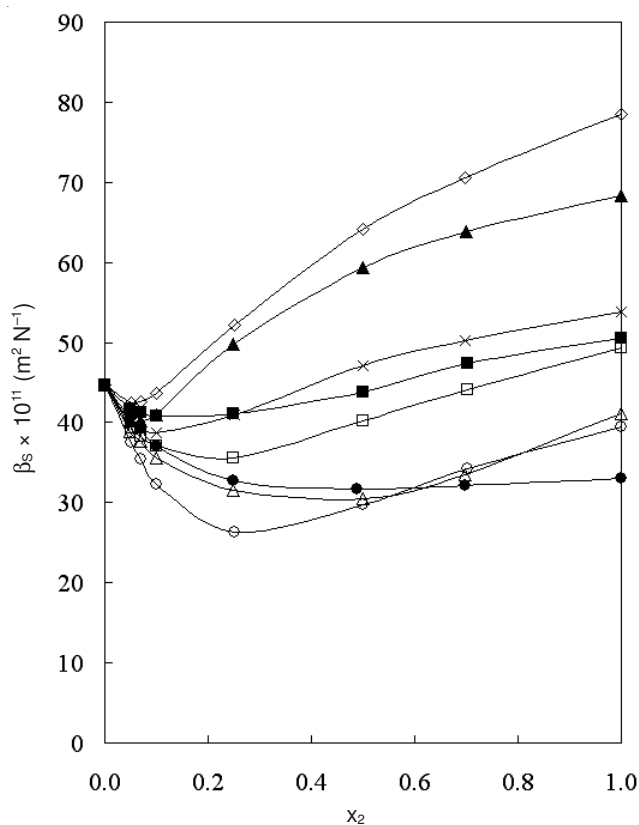


Fig. 3. Variation of isentropic compressibilities (β_s) with mole fraction of solute x_2 for aqueous systems at 298.15K: \diamond - \diamond , ACN; \square - \square , DMF; Δ - Δ , DMSO; \times - \times , DO; \circ - \circ , EDA; \bullet - \bullet , EG; \blacksquare - \blacksquare , PY; \blacktriangle - \blacktriangle , THF

between solute and solvent molecules must be taking place at minimum of the $\phi_s - x_2$ curves. Same types of results have been obtained for these systems at lower temperatures¹³⁻¹⁵.

Fig. 4 represents the variations of apparent molar volume of the solute (ϕ_v) as a function of mole fraction of solute (x_2) at 298.15 K for all the aqueous systems. It is observed from the above figure that for ACN + H₂O, THF + H₂O, DO + H₂O and PY + H₂O systems the values of ϕ_v increase continuously with increase in concentration of solute. However, initial slopes of $\phi_v - x_2$ curves for first three systems are different. It is observed that the slopes of the curves for these systems are more positive initially and become less positive with increase in concentration of the solute. This suggests that strong solute-solvent/solute-solute interactions are taking place initially and after that (small positive slopes) usual solute-solute interactions dominate. The slope of PY + H₂O system remains almost same indicating uniform solute-solute interactions. Since, we did not study these systems in a really low concentration region, we are not in a position to comment firmly on whether at lower concentrations solute-solvent interactions are taking place or solute-solute interactions are taking place. For EG + H₂O, EDA + H₂O, DMSO + H₂O and DMF + H₂O systems values initially decrease with increase in concentration of the solute up to certain concentration go through flat minima and again increase with concentration of the solute. The initial negative slopes of $\phi_v - x_2$ curves suggest induced solvent-solvent interactions because of overlap of the co-sphere¹⁴ water molecules. Same types of observations have been made at lower temperatures for aqueous solutions of EG, DMF, ACN, DO, DMSO and EDA¹³⁻¹⁵. However in case of aqueous solutions of THF a flat minimum is observed at lower temperatures. The positive slopes of $\phi_v - x_2$ curves after minima suggest usual solute-solute interactions. Woolley and coworkers observed that the apparent molar volumes of DO, DMSO and THF are independent of concentration of solute in aqueous solutions in the 0-3 m concentration range at a particular temperature and at 0.35 MPa and the values increase with increase in temperature³⁰. It suggests that at lower concentration of these solutes only solute-solvent interactions are prevalent. It is observed from Tables 2 and 3 that at 308.15 K the values of ϕ_v are higher than at 298.15 K at a particular concentration for that particular aqueous system. This happens because of the fact that with increase in temperature water molecules around the solute molecule are loosely bound, that result in increase in apparent molar volume of the solute.

Table-4 comprised the values of limiting apparent molar volumes of the solute ($\phi_v^0 = \bar{V}_2^0$, where \bar{V}_2^0 is limiting partial molar volume of the solute) at 298.15 and 308.15 K. It is seen that the values of ϕ_v^0 increase with increase in temperature. The values of temperature coefficient of ϕ_v^0 ($\phi_E^0 = d\phi_v^0/dT$) at 303.15 K are also collected in Table-4. It is observed from the Table-4 that all the values of ϕ_E^0 are positive. The lowest value of ϕ_E^0 is observed for EDA and highest value is observed for DMSO. The lower values ϕ_E^0 for EDA and EG suggest that water around these molecules is less susceptible to temperature. It might be because of the fact that these molecules are accommodated in the cavities of water structure and so no temperature effect is seen on the structure of water surrounded

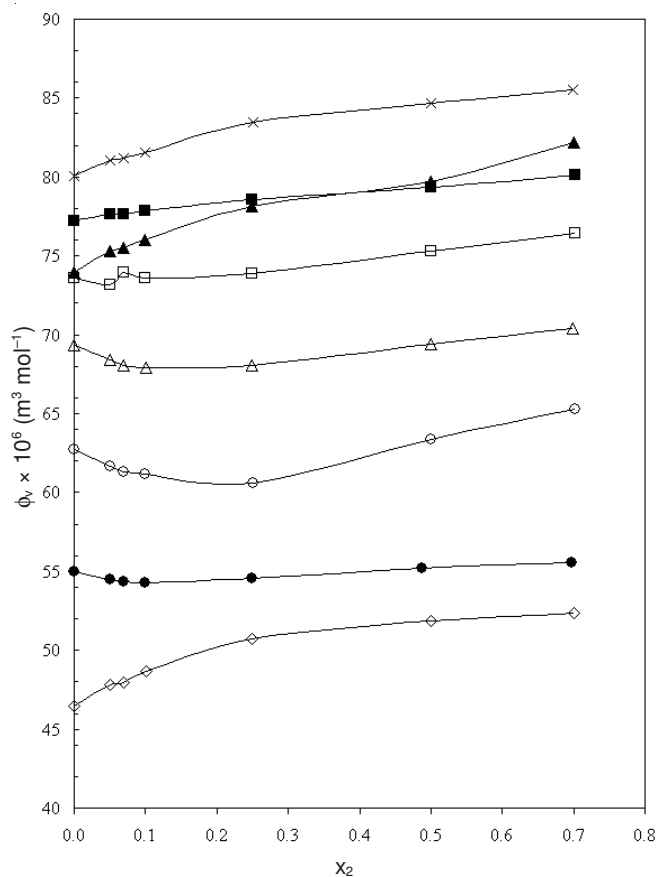


Fig. 4. Variation of apparent molar volume (ϕ_v) of solute with mole fraction of solute x_2 for aqueous systems at 298.15K: \diamond - \diamond , ACN; \square - \square , DMF; Δ - Δ , DMSO; \times - \times , DO; \circ - \circ , EDA; \bullet - \bullet , EG; \blacksquare - \blacksquare , PY; \blacktriangle - \blacktriangle , THF

around the solute molecules. In fact, the temperature coefficient

$$\text{of } \phi_{v,E}^0, \frac{d\phi_{v,E}^0}{dT} = \frac{d^2\bar{V}_2^0}{dT^2}, \text{ can be used to ascertain whether the}$$

solute is structure making or structure breaking³¹. Unfortunately, we have no data at three temperatures and so, on the basis of the present data it is difficult to judge whether a particular solute is structure making or structure breaking.

Fig. 5 showed plotted the variations of apparent molar isentropic compressibilities of solutes (ϕ_{KS}) against mole fractions of solutes (x_2) for aqueous solutions of solutes at 298.15 K. The scrutiny of the above figure reveals that ϕ_{KS} values increase with increase in concentration of the solute. However, the positive slopes of the $\phi_{KS} - x_2$ curves initially at lower concentrations are high and after certain concentration of the solute the curves flatten off. The initial slope is highest for THF + H₂O system and it is lowest for EG + H₂O system. The lowest slope for EG + H₂O system suggests that EG molecules dissolve in to water without disturbing the existing water structure or EG molecules are compatible with the water structure. The flattening of $\phi_{KS} - x_2$ of the curves at higher concentration might be due to less availability of structured water molecules at higher concentration of the solute. Moreover, the values of ϕ_{KS} increase with increase in temperature for all the solutes at a given concentration. This might be happening due to that fact that as the temperature increases the water-solute bonded structure gets loosened¹⁴.

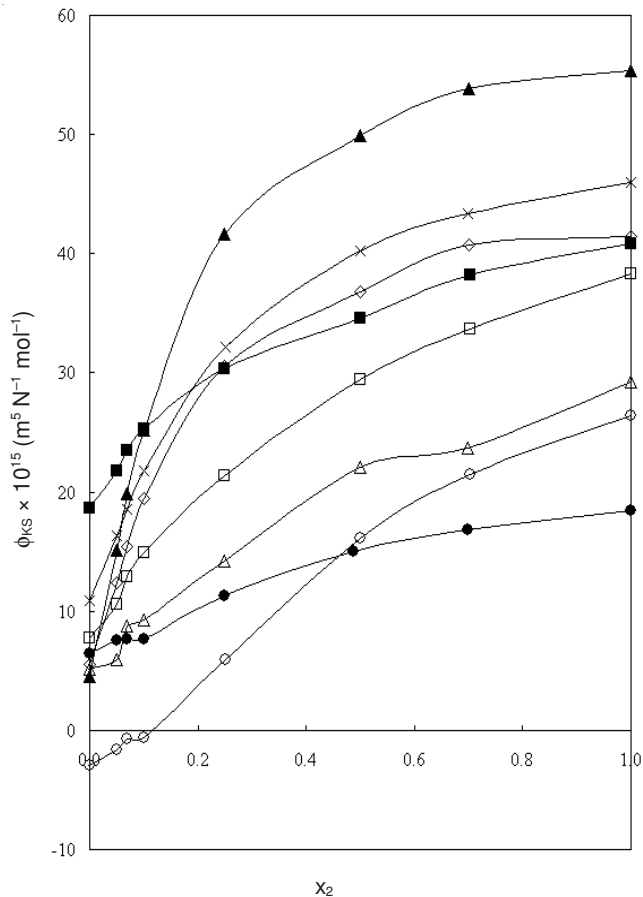


Fig. 5. Variation of apparent molar isentropic compressibility (ϕ_{KS}) of solute with mole fraction of solute x_2 for aqueous systems at 298.15K: \diamond - \diamond , ACN; \square - \square , DMF; Δ - Δ , DMSO; \times - \times , DO; \circ - \circ , EDA; \bullet - \bullet , EG; \blacksquare - \blacksquare , PY; \blacktriangle - \blacktriangle , THF

The values of limiting apparent molar isentropic compressibilities of solutes (ϕ_{KS}^0) at 298.15 and 308.15 K are given in Table-4. It is seen that the values of ϕ_{KS}^0 are positive for all the solutes except for EDA. For solutes namely DMF, THF, ACN, DMSO and EG the values of ϕ_{KS}^0 are of same order. Where as for pyridine it is quite high ($18.62 \times 10^{-15} \text{ m}^5 \text{ N}^{-1} \text{ mol}^{-1}$) and for DO it is $10.89 \times 10^{-15} \text{ m}^5 \text{ N}^{-1} \text{ mol}^{-1}$. For EDA it is small negative. It is known that ϕ_{KS}^0 is a measure of protection that solute gives to solvent structure³. The small negative value of ϕ_{KS}^0 for EDA suggests that when EDA is dissolved in water, it is accommodated in the cavities of water structure without disturbing the existing water structure. This corroborates well with present observation. Recall that ϕ_{KS} is basically a measure of change in apparent molar volume with change in pressure. Seen in this context, the small positive values of ϕ_{KS}^0 for DMF, THF, ACN, DMSO and EG suggest that the water around these solutes is less compressible as compared to water around DO and PY. It is further observed from close scrutiny of Table-4 that ϕ_{KS}^0 values increase with increase in temperature. Table-4 are also collected the value of temperature coefficient of ϕ_{KS}^0 i.e., ϕ_{KS}^0/dT . It is observed that the value of $d\phi_{KS}^0/dT$ is smallest for EG and it is maximum for DMF. Thus it can be concluded that water around EG molecule is less sensitive to temperature as compared to other solutes.

ACKNOWLEDGEMENTS

One of the authors (AAB) is thankful to CSIR, New Delhi for awarding Emeritus Scientistship (ES Scheme No.21(0695)/07/EMR-II). BRT is also thankful to UGC New Delhi for awarding FIP fellowship and financial assistance.

REFERENCES

1. F. Franks, *Water a Comprehensive Treatise*, Plenum press New York, Vol. 2 (1973).
2. J.L. Neal and D.A.I. Goring, *J. Phys. Chem.*, **74**, 658 (1970).
3. F. Franks, J.R. Ravenhill and D.S. Reid, *J. Sol. Chem.*, **1**, 3 (1972).
4. S. Kabani, G. Conti and E. Matteoli, *J. Sol. Chem.*, **5**, 751 (1976).
5. G.C. Benson and O. Kiyohara, *J. Sol. Chem.*, **9**, 791 (1980).
6. M.V. Kaulgud and K.J. Patil, *J. Phys. Chem.*, **78**, 714 (1974).
7. M.V. Kaulgud and K.J. Patil, *J. Phy. Chem.*, **80**, 138 (1974).
8. M.V. Kaulgud and K.S.M. Rao, *J. Chem. Soc. Faraday Tans. 1*, **75**, 2237 (1979).
9. M.V. Kaulgud and S.S. Dhondge, *Ind. J. Chem.*, **27A**, 6 (1988).
10. M.V. Kaulgud, A. Shrivastava and V.K. Mate, *Ind. J. Chem.*, **30A**, 834 (1991).
11. M.V. Kaulgud, S.S. Dhondge and A.G. Moharil, *Ind. J. Chem.*, **34A**, 106 (1995).
12. M.V. Kaulgud, A.G. Moharil and S.S. Dhondge, *Ind. J. Chem.*, **35A**, 746 (1996).
13. L. Ramesh, S.S. Dhondge and M.N. Ray, *Ind. J. Chem.*, **38A**, 70 (1999).
14. S.S. Dhondge and L. Ramesh, *J. Chem. Thermodyn.*, **39**, 667 (2007).
15. S.S. Dhondge, C.P. Pandhurnekar and L. Ramesh, *J. Chem. Thermodyn.*, **40**, 1 (2008).
16. J.A. Riddick and W.B. Bunger, *Techniques of Chemistry-Organic Solvents*, Wiley Interscience, NY (1970).
17. J.G. Baragi, M.I. Aralaguppi, T.M. Aminabhavi, M.Y. Ariduraganavar and A.S. Kittur, *J. Chem. Eng. Data*, **50**, 910 (2005).
18. M.A. Saleh, M.S. Ahmed and M.S. Islam, *Phys. Chem. Liq.*, **40**, 477 (2002).
19. J.N. Nayak, M.I. Aralaguppi, U.S. Toti and T.M. Aminabhavi, *J. Chem. Eng. Data*, **48**, 1483 (2003).
20. S.K. Mehta and R.K. Chauhan, *J. Sol. Chem.*, **26**, 295 (1997).
21. M.I. Aralaguppi, C.V. Jadar and T.M. Aminabhavi, *J. Chem. Eng. Data*, **41**, 1307 (1996).
22. T.M. Aminabhavi and K. Banerjee, *J. Chem. Eng. Data*, **43**, 852 (1998).
23. F. Comelli, R. Francesconi, A. Bigi and K. Rubini, *J. Chem. Eng. Data*, **51**, 1711 (2006).
24. J.A. Riddick and W.B. Bunger, *Organic Solvents, Physical Properties and Methods of Purification Techniques of Chemistry*, Wiley-Interscience, New York, Vol. 2, edn. 3.
25. C. Yang, P. Ma, F. Jing and D. Tang, *J. Chem. Eng. Data*, **48**, 836 (2003).
26. O. Kiyohara, P.J.D. Arcy and G.C. Benson, *Can. J. Chem.*, **57**, 1006 (1979).
27. S.K. Kushare, R.R. Kolhapurkar, D.H. Dagade and K.J. Patil, *J. Chem. Eng. Data*, **51**, 1617 (2006).
28. F.J. Millero, *J. Phys. Chem.*, **74**, 356 (1970).
29. V.A. Del Grosso and C.W. Mader, *J. Accost. Soc. Am.*, **5**, 1442 (1972).
30. D.M. Swenson, M.B. Blodgett, S.P. Ziemer and E.M. Woolley, *J. Chem. Thermodyn.*, **40**, 248 (2008).
31. L.G. Hepler, *Can. J. Chem.*, **47**, 4613 (1969).